Polymer 105 (2016) 227–233

Contents lists available at ScienceDirect

Polymer

journal homepage: www.elsevier.com/locate/polymer

Deformation of polyurea: Where does the energy go?

P.H. Mott [a, *], C.B. Giller [b, 1], D. Fragiadakis [a], D.A. Rosenberg [a, 2], C.M. Roland [a]

[a] Chemistry Division, US Naval Research Laboratory, Washington DC, 20375-5342, United States
[b] Leidos Inc., 11951 Freedom Drive, Reston, VA 20190, United States

ARTICLE INFO

Article history:
Received 20 June 2016
Received in revised form
7 October 2016
Accepted 12 October 2016
Available online 13 October 2016

Keywords:
Polyurea
Thermoelasticity
High strain rate

ABSTRACT

Infrared thermography was carried out on a polyurea, stretched to failure, over four decades of strain rates (0.026–400 s^{-1}). A correction for convective heat transfer was developed that enabled the thermal response of slower experiments to be compared to adiabatic measurements. Overall the deformation was exothermic, but in contrast to simple, homogeneous elastomers, the temperature change was a complicated function of strain and rate. The largest temperature rise was 20 °C, which in comparison to other rubbers (e.g., natural and styrene butadiene rubber, both neat and reinforced with filler), is about twice that at failure and 5–10 times that at comparable strains. These temperature changes in the polyurea correspond to a half decade shift toward higher frequency of the soft segment dynamics. At low rates (<1 s^{-1}), the temperature increased up to a strain of *ca.* 3, with the subsequent decline corresponding to an upturn in the stress. At high strain rates (>1 s^{-1}), the temperature increased monotonically. For samples stretched to failure, there was a maximum in the temperature increase versus strain rate at an intermediate rate = 1.2 s^{-1}, due to the competing effects of greater heat generation and lower failure strain. Thermoelastic inversion was observed at low rates at *ca.* 4% strain, consistent with the thermal expansion coefficient, indicating that entropic elasticity is a dominant mechanism at low strains. However, at higher strains the deformation departs from this behavior, with endothermic processes commencing as the material begins to yield. These processes are identified with plastic deformation and breakup of the hard domains within the phase-separated polyurea structure. An energy balance indicates that, notwithstanding the large temperature increases, structural changes account for the largest part of the strain energy.

Published by Elsevier Ltd.

1. Introduction

Elastomeric polyurea is a versatile material that finds applications as a coating for storage tanks, military armor, roofs, parking decks, ships, and truck bed-liners, etc. It is a segmented block copolymer having an ideal morphology for mechanical properties: isocyanate-rich segments self-assembled via hydrogen bonds into nano-scale domains that have a glass-transition temperature, T_g, well above ambient. These hard domains are embedded in a continuous matrix of polyamine soft segments that contain some admixed hard segments. The microphase-separated hard domains are connected to the matrix through the continuity of the chains. When subjected to tensile deformation, the polyurea exhibits yielding, followed by a large upturn in the stress [1,2]. The consequent large energy dissipation, reflecting a large internal friction and irreversible structural changes, provides superior toughness. Good mechanical performance is also obtained at higher strain rates (e.g., impact), when the perturbation frequency falls within the range of the polyurea segmental dynamics [3]. Most rubbery polymers have lower T_g, so that the segmental dynamics are too high in frequency to absorb energy from high strain rate deformations. When used as a coating on metal substrates, in addition to substantial energy absorption, mechanisms that improve the impact resistance include delay of the onset of necking of the substrate [4] and lateral spreading of the impact force [5]. These appear to be a consequence of the transient hardening induced by impact [3,6].

For slow deformations through the yield point, the hard domains align, concentrating strain in the continuous phase. As the stress increases, the domains fully align parallel to the stretch

* Corresponding author.
E-mail address: peter.mott@nrl.navy.mil (P.H. Mott).
[1] Current address: MITRE Corporation, McLean VA 22102, United States.
[2] Current address: Federal Energy Regulatory Commission, Office of Energy Projects, Washington DC 20426, United States.

http://dx.doi.org/10.1016/j.polymer.2016.10.029
0032-3861/Published by Elsevier Ltd.

direction [7,8]. When failure is imminent, the hard domains and their interface with the matrix are disrupted, with this local damage reflected in permanent set (incomplete recovery) [9]. However at higher rates, the stress upturn is absent and disruption of the hard domains is avoided; consequently, sample recovery is nearly complete [9]. Our interest in elastomeric polyurea arises from its application as a coating to enhance the blast and ballistic performance of armor [3,5]. The aim of the work was to determine how the strain energy is distributed among viscoelastic dissipation (heat), stored elastic energy, and the work of irreversible structural changes. The distribution of energy and its dependence on strain rate are critical aspects of impact toughness and performance in armor applications.

High speed thermography was employed to measure instantaneous temperature changes in the deformed polymer; this method was unavailable in earlier studies of rubber thermoelasticity [10,11]. Thermography provides a temperature map, important for detection of microstructural changes near flaws [12–15]. Recent studies of heat dissipation in rubber have addressed non-linear modeling [16,17], crystallization kinetics [18,19], and the Mullins effect [20]. Conversely, thermomechanical investigations of more complex materials, including filled rubber [21,22], are scarce. Herein we apply this approach to polyurea, an elastomer with a complex microstructure.

2. Experimental

The polyurea was formed by reaction of a modified diphenylmethane diisocyanate (Isonate 143L from Dow Chemical; 1.21 g/ml, 144 g/eq) with an oligomeric polydiamine (Versalink P1000 from Air Products; 1.04 g/ml, 600 g/eq). The volume mixing ratio was 1:4 isocyanate to diamine; post-curing for 12 h at 80 °C completes the reaction. The resulting material has *ca.* 35% hard and 65% soft domains by weight [23]. The components were vacuum degassed prior to mixing, and then cast using a cartridge plunger into ~1 mm thick sheets. Test specimens (ASTM D4482) were all die cut from the same cured sheet.

The high speed testing was carried out using a custom instrument [24]. Briefly, a drop-weight tester is used to rapidly stretch the sample, with the stress determined from the measured load after correcting for inertia, and the strain deduced from the displacement of fiducial marks recorded with a camera (Vision Research Phantom 7 monochrome, 20 kHz frame rate, 800 × 120 pixel resolution). Conventional low speed testing, at strain rates up to 0.2 s^{-1}, employed an Instron 5500R with optical extensometer. All tests were done at ambient temperature.

The temperature of deforming samples were measured using a FLIR SC6811 infrared camera (1093 Hz frame rate, 640 × 32 resolution), synchronized with the video recording of the strain (fiducial marks were detected by the IR camera). Typical thermograms are shown in Fig. 1. The camera detects 3–5 μm wavelength light with the radiant emittance determined from calibrated intensities. Only temperature changes (differences from the sample surroundings) are reported herein; the uncertainty of the measured temperature changes was 0.03 deg. The values reported herein are averages over the sample gauge section. The latter, as seen in Fig. 1, contracts laterally during extension, so that the measured region is only a few pixels wide just prior to failure. Any measurements exhibiting "hot spots", due to sample heterogeneities, were discarded.

3. Convective heat loss correction

Heat loss to the surroundings causes the measured sample temperature change θ_M to deviate from the adiabatic temperature change θ as

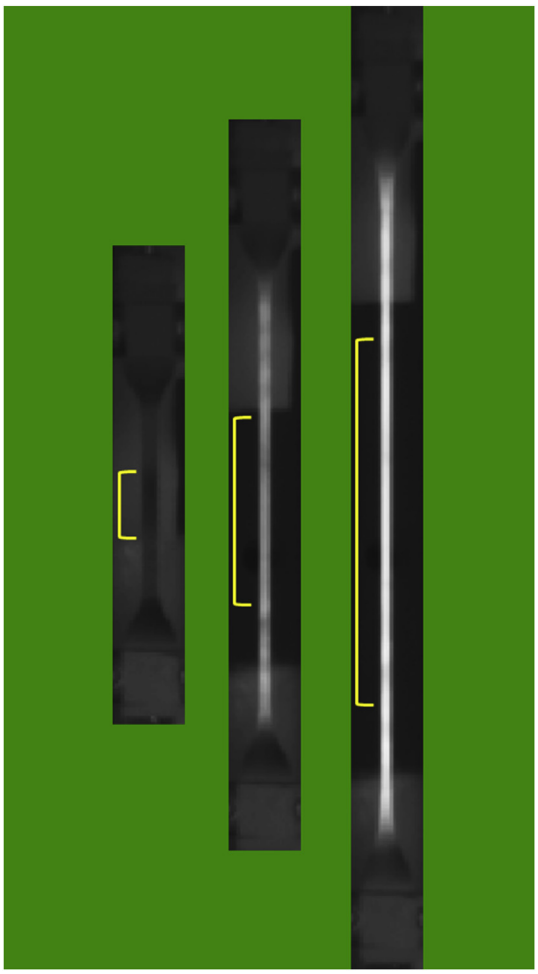

Fig. 1. Representative thermographs at $\lambda = 1$, 2.23, and 3.21. The temperature range is from 15 °C (black) to 60 °C (white), on a linear scale. Brackets identify the approximate area over which the measurements were averaged. Fiducial marks may be seen in the center image, which are the slight intensity modulations along the gauge section outside of the bracket.

$$\theta = \theta_M + \theta_C \tag{1}$$

where θ_C is the change due to convection. Of course at sufficiently short times this heat loss is negligible ($\theta_C = 0$); for longer times, the following procedure was developed to account for non-adiabatic conditions.

Consider a thin rubber sample that has been rapidly and uniformly heated by stretching, then held immobile during cooling to ambient temperature. Assuming negligible thermal gradients within the sample (as justified below) and no heat production from structural or chemical changes, the rate of heat lost by convection is

$$\frac{dQ}{dt} = -\frac{dU}{dt}, \tag{2}$$

where dU/dt is the rate of change in the internal energy of the rubber. The convective heat transfer rate is

$$\frac{dQ}{dt} = A_S h \theta_M(t), \tag{3}$$

where A_S is the convective surface area, $= 2L(w + d)$, with L, w, and

d the respective sample length, width and depth (in the rubbery regime polyurea is essentially incompressible [25]); h is the convective heat transfer coefficient; and θ_M (t) is the actual (i.e., measured) temperature difference from the surroundings. The internal energy derivative is

$$\frac{dU}{dt} = \rho VC\frac{dT}{dt}, \tag{4}$$

where ρ, V, C, and T are the respective density, volume, heat capacity, and temperature. Combining the above and using $dT = d\theta$, eq. (2) is integrated to find the fractional change in temperature

$$\frac{\theta_M(t)}{\theta_i} = \exp\left(-\frac{A_S ht}{\rho CV}\right) = \exp\left(-\frac{t}{\tau}\right), \tag{5}$$

where θ_i is the initial temperature change and τ a time constant characteristic of the material and its surroundings.

Equation (5) was used to determine h in a static cooling experiment. A test piece was quickly deformed to a stretch ratio $\lambda = 3$ and then retracted to $\lambda = 1$, with the ensuing temperature decay measured. The average of five trials was used to compute h, using $C = 0.42$ J g^{-1} K^{-1} and $\rho = 1.04$ g cm^{-3} [23,26]; the result was $h = 8.1 \pm 1.7$ W m^{-2} K^{-1}. The measurement assumes that heat generation during the static (load-free) cooling is negligible, even though the sample is slowly recovering strain. The assumption was corroborated by a separate measurement of h for a heated but unstretched sample, which yielded the same results within uncertainty.

For a thin rubber sample undergoing uniaxial strain, equation (2) is valid, but the convective surface area in eq. (3) changes with time; thus,

$$A_S(t) = [\lambda(t)]^{1/2}A_{S0} = 2[\lambda(t)]^{1/2}L_0(w_0 + d_0), \tag{6}$$

which assumes isochoric conditions. The subscript "0" denotes the original (undeformed) value. The total convective heat lost for a time t_A is found by integrating eq. (3):

$$Q(t_A) = \int_0^{t_A}\frac{dQ}{dt}dt = hA_{S0}\int_0^{t_A}[\lambda(t)]^{1/2}\theta_M(t)dt. \tag{7}$$

The change in sample temperature due to convection is

$$\theta_C(t_A) = \frac{Q(t_A)}{\rho CV} = \frac{hA_{S0}}{\rho CV}\int_0^{t_A}[\lambda(t)]^{1/2}\theta_M(t)dt. \tag{8}$$

Thus, the area under $[\lambda(t)^{1/2}\ \theta_M\ (t)]$ accounts for the effects of changing shape and temperature differences on the heat transfer from the rubber to its surroundings.

Fig. 2 plots the measured and adiabatic temperature differences for two strain rates. Initially the difference between θ_M and θ is negligible. The correction depends on the temperature difference with the surroundings, which becomes significant sooner at the higher strain rate (1.2 s^{-1}). The inset shows the normalized convective loss, $= \theta_C/\theta$, just prior to mechanical failure, as a function of measurement time. Over the initial 3s, the convective heat loss accounts for less than 3% of the total thermal energy, evaluated as

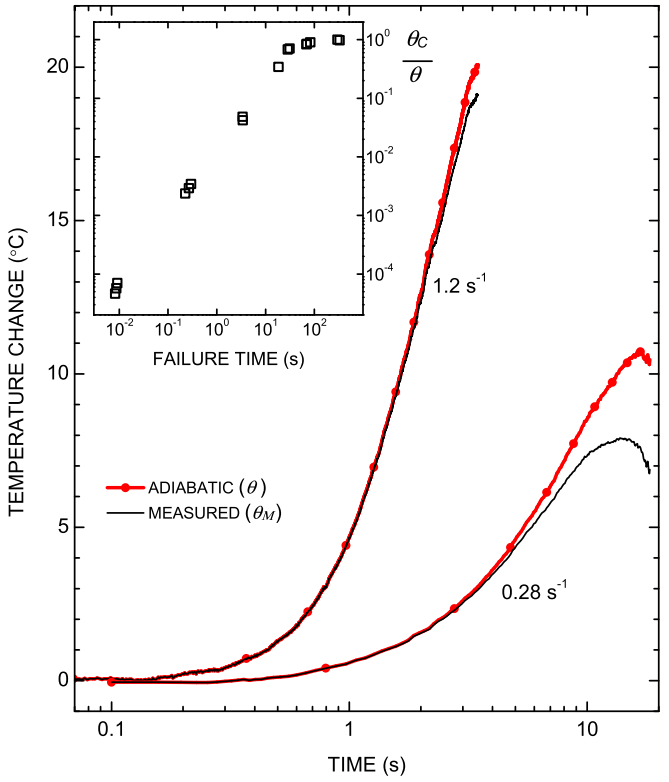

Fig. 2. Measured and adiabatic temperature change (i.e., difference from the surroundings) for two tests at the indicated strain rates. The behavior is essentially adiabatic up through *ca.* 3 s. Inset: convective temperature change normalized by the adiabatic temperature change, measured at failure; each datum is for a different strain rate.

$$W_{heat}(t_A) = \rho VC\int_0^{t_A}\frac{dT}{dt}dt\,, \tag{9}$$

after the adiabatic correction has been applied. This is in good agreement with previous observations [11]. Our analysis assumes that the coefficient h remains constant over the tested range of strain rates, which assumes the test equipment does not perturb the air near the sample. Since the convective heat transfer is proportional to time, exponentially increasing the rate will decrease the test time in inverse proportion, whereby a measurement will approach the adiabatic ideal to within the temperature uncertainty.

The forgoing analysis assumes that the heat transfer is governed only by convection; i.e., that thermal diffusion within the sample is "fast." This is justified by the small Biot number [27]

$$\mathrm{Bi} = \frac{hL_c}{k}, \tag{10}$$

where k is the thermal conductivity and L_c is a characteristic length, taken here as one-half the sample thickness. Convective systems with low Biot numbers can be modelled as having uniform temperature. An analysis of this approximation for various shapes with Bi = 0.1 showed that the largest temperature deviation is within 2% of the mean temperature difference [28]. The thermal conductivity for polyurea is unavailable, but using the value for the chemically similar polyurethane, $k = 0.29$ Wm^{-1}K^{-1} [29], the Biot number for the present measurements is ~0.02, well below the threshold for significant thermal gradients.

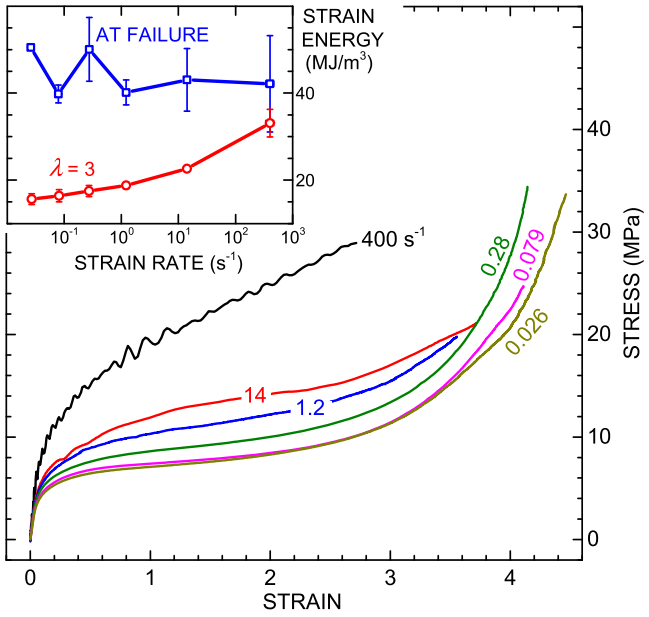

Fig. 3. Representative engineering stress-strain curves at the indicated strain rate. Inset: strain energy density at $\lambda = 3$ and at failure. Points are averages of two or three trials, with error bars denoting the scatter.

4. Results and discussion

Representative engineering stress-strain curves encompassing four decades of strain rate are shown in Fig. 3. The data are in accord with previous results for polyurea, showing a yield point and subsequent upturn at $\lambda > 4$, along with a weak sensitivity to strain rate [1,2]. The inset shows the dependence on strain rate of the strain energy density at an intermediate extension ($\lambda = 3$) and at failure. At intermediate strain there is a monotonic increase, while at failure, there is no discernable rate-dependence. The latter reflects the countervailing effect of the decrease in failure strain with increasing strain rate.

The adiabatic temperature changes for the measurements in Fig. 3 are shown in Fig. 4. The largest increase was 20 °C, which is five to ten times larger than the temperature rise at comparable strains and rates reported for gum (unfilled) elastomers such as natural rubber [10,11,16–18], polychloroprene [10], and styrene-butadiene rubber [20,30]. The temperature increase is also significantly larger than for filled natural, butadiene, and styrene-butadiene rubbers, with filler concentrations similar to the hard segment content of the polyurea (35%) [21,22]. The difference can be ascribed to the high internal friction coefficient of polyurea, resulting from extensive H-bonding and a high T_g. Some observations drawn from Fig. 4: (i) As shown in the inset, the behavior is endothermic for the lower strain rates at strains < 0.1. (ii) The left (main) plot shows that the temperature levels off, and then decreases, at high strains. (iii) From the right plot the maximum exothermic change can be seen to occur at the intermediate strain rate of 1.2 s^{-1}.

The initially endothermic behavior at the two lowest strain rates (*ca.* 0.06 °C drop at 0.04 strain in Fig. 4) is the well-known thermoelastic inversion [31–34], representing the competition between thermal expansion and entropic elasticity. The stretch ratio for which the minimum in θ occurs is related to the coefficient of thermal expansion α by [33]

$$\lambda_{inv} \approx (1 + 3\alpha T)^{1/3}. \quad (11)$$

Using the published value of α for polyurea [35], 14×10^{-5} K^{-1}, gives $\lambda_{inv} = 1.041$, in agreement with the minimum in Fig. 4. At the 0.28 s^{-1} rate, the temperature minimum becomes shallower and shifts to lower strains. At higher rates a minimum is not detected within the resolution of the measurements. This suggests that at higher rates, processes other than thermal expansion and entropic elasticity contribute to the temperature change.

The second behavior of note, the negative temperature change at high strain, may be distinguished by the downturn beginning at λ ~4.4 in the curve for 0.28 s^{-1} (denoted by an arrow in Fig. 4). This feature is reproducible, with similar breaks in θ observed at low and intermediate rates, but not at the higher strain rates, 14 and 400 s^{-1}. As seen by comparison to Fig. 3, this decrease in θ occurs at the

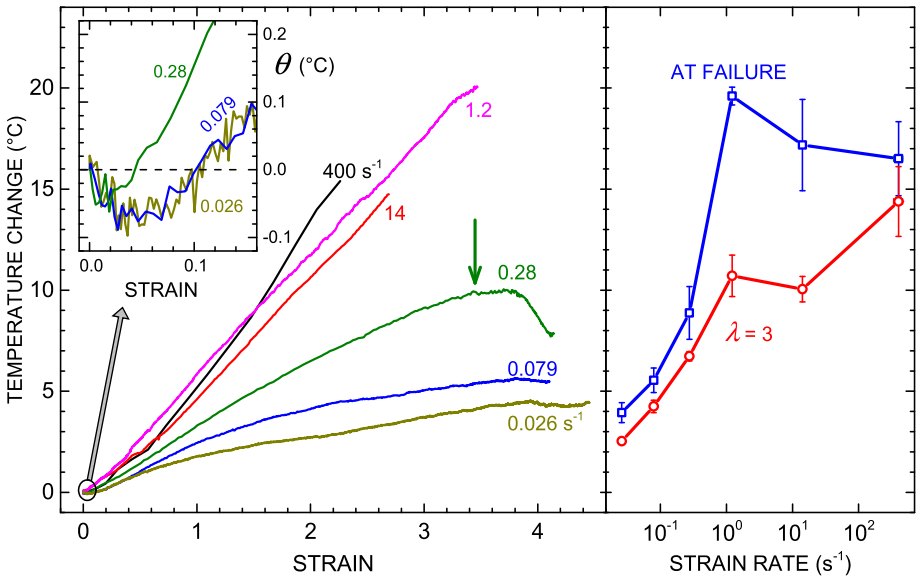

Fig. 4. Left plot: Adiabatic temperature change, θ, for the deformation measurements in Fig. 3 (strain rates indicated). The arrow identifies the onset of an endothermic break in the curve for 0.28 s^{-1}, as discussed in the text. Inset: low strain data on an expanded scale, showing the temperature minimum. Right plot: θ as a function of strain rate at $\lambda = 3$ and at failure; error bars are the data range.

strain associated with the prominent stress upturn. The stress upturn is absent at high strain rates, as is the change in the temperature behavior. *In-situ* microstructural studies have associated the stress upturn to the breakup of the hard domains [7,8]; the results herein show that this breakup is sufficiently endothermic to overwhelm the strong exothermic stress-strain behavior. The third observation, that the maximum exothermic change occurs at an intermediate strain rate = 1.2 s^{-1}, identifies the rate associated with the maximum in these microstructural changes. This aspect of the behavior requires further study.

In Fig. 5 is plotted the fraction of strain energy density manifested as heat for the same set of measurements. The low strain ($\lambda < 1.1$) endothermic behavior has been excluded from this figure due to the large experimental scatter. The curves reach a maximum at λ ~1.4, with a steady decline afterward. At extensions associated with the upturn in the stress ($\lambda > 4$), the decrease in (relative) thermal energy accelerates, giving rise to the changed behavior of θ noted above. If deformation were governed purely by entropic elasticity, the evolved temperatures in Fig. 4 would be concave upward, and the fractional strain energy in Fig. 5 would be constant [31,33,36]. This is approximately the case for the highest rate (400 s^{-1}), which has neither a sharp yield point nor a stress upturn (Fig. 3). In contrast when deformed at slower rates, the structural changes that underlie yielding and the stress upturn cause a net endothermic response.

Insight into the mechanical behavior can be gleaned from dielectric relaxation measurements. A dispersion in the dielectric loss occurs at frequencies corresponding to the segmental dynamics. The temperature-dependence of the frequency of this loss peak, f_{max}, follows the Vogel-Fulcher equation [37,38]

$$\log f_{max} = \log f_0 - \frac{B}{T - T_0}, \tag{12}$$

in which B, T_0, and f_0 are constants. For the soft segment domains of polyurea, a fit of eq. (12) to the T-dependence of the loss peak gives B = 686.1 K, T_0 = 160.2 K, and f_0 = 96.1 GHz [3]. Using eq. (12) we calculate that the 15 °C temperature increase during the 400 s^{-1} experiment would shift the relaxation spectrum 0.47 decades higher in frequency. This enhances the chain mobility during the course of the stretching.

We can assess how the strain energy is distributed among heat, structural changes, and recoverable deformation. The total strain energy and recovered energy were determined from

$$W_{strain} = \int_0^{\varepsilon_{max}} \sigma_{load} d\varepsilon \tag{13}$$

$$W_{recv} = \int_{\varepsilon_{max}}^{0} \sigma_{recv} d\varepsilon \tag{14}$$

where σ_{load} and σ_{recv} are the respective loading and retraction stress, and ε_{max} is the maximum strain. (Retraction was measured in separate hysteresis experiments, limited to low rates.) The structural energy W_{struct}, responsible for any alterations of the phase morphology and the interfacial material, was found by subtracting the thermal energy W_{heat} and recovered energy W_{recv} from the total energy W_{strain} [39]:

$$W_{struct} = W_{strain} - W_{recv} - W_{heat}. \tag{15}$$

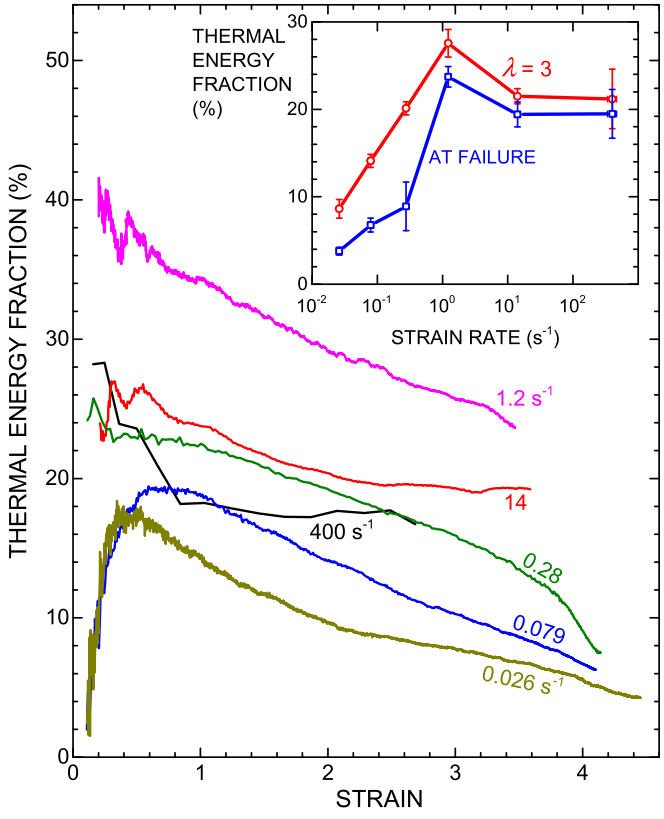

Fig. 5. Thermal energy density normalized by the total strain energy density (from data in Figs. 3 and 4). Inset: Same results as a function of strain rate for λ = 3 and at failure. Points are averages of two or three trials, and error bars denoting the range.

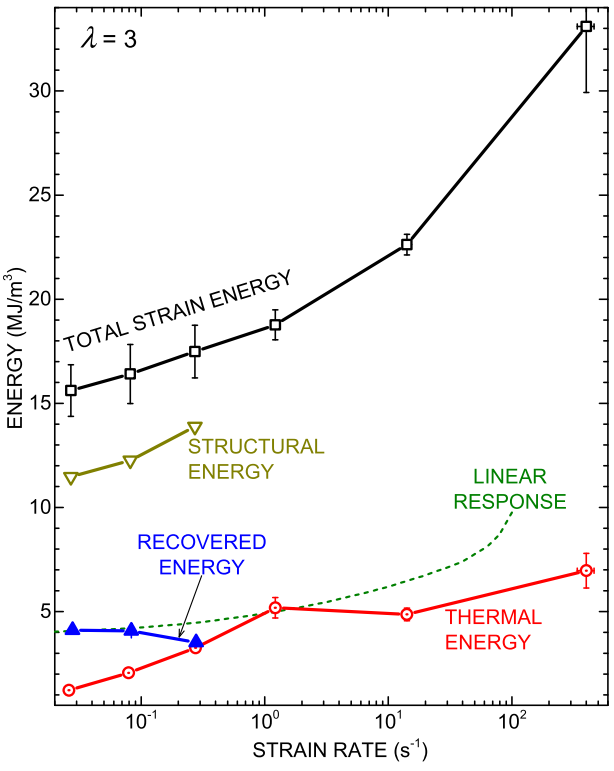

Fig. 6. Rate dependence of the total strain energy density and the various contributions for λ = 3; error bars are the standard deviation. The dashed line represents the linear strain energy density calculated from low strain dynamic mechanical measurements (eq. (14)).

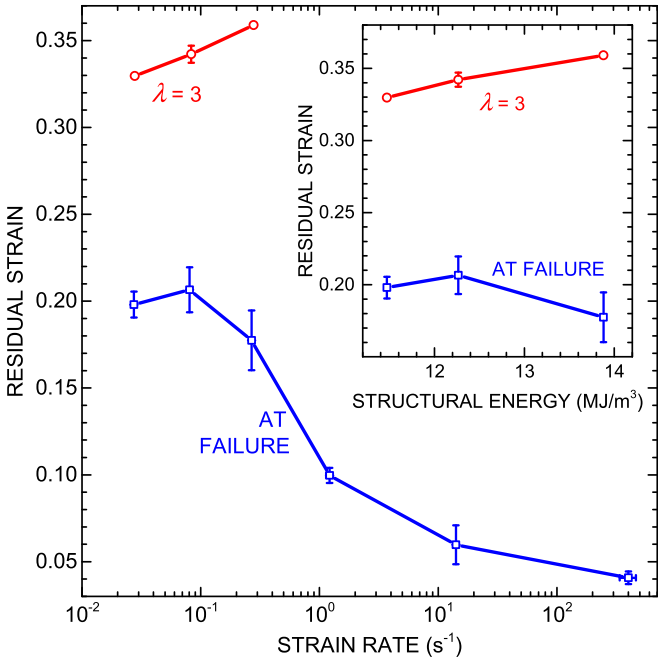

Fig. 7. Residual strain measured at $\lambda = 3$ and at failure as a function of strain rate. Inset: residual strain plotted versus the structural strain energy (see text).

The results are plotted in Fig. 6 for $\lambda = 3$, where it can be seen that disruption of the polyurea structure causes the greatest resistance to deformation. This contributes to the toughness of the material and is quite different behavior from gum elastomers such as natural rubber, styrene-butadiene rubber, polybutadiene, polychloroprene, and polydimethyl siloxane. Absent strain-crystallization, almost complete energy recovery is observed for these materials [40,41]. The bulk of their strain energy (70–100%) is manifested as heat, with very little consumed by structural changes (typically 0–40% of the input strain energy) [36]. In distinction, polyurea exhibits large temperature increases related to its large internal friction, coupled with substantial energy loss (as much as 75%) due to deformation and breakup of the phase-segregated morphology. At higher strain rates the disruption of the interfacial material between the hard domains and the matrix becomes negligible, resulting in net exothermic behavior. This is consistent with the minimal permanent set observed at high strain rates, as seen in Fig. 7 showing the variation of residual strain with rate. (The values measured after failure are lower in part because these were obtained several weeks after testing, whereas the $\lambda = 3$ measurements were made immediately after unloading.) The inset shows the correlation of residual strain with the structural energy. Note the data for $\lambda = 3$ have an intercept at zero, corroborating that the structural changes indeed underlie the portion of the strain energy ascribed to it. Similar rate-dependent permanent set in polyurea was reported previously [9].

The results in Fig. 6 emphasize the very non-linear character of the material response. Another gauge of this is to compare the strain energy density calculated from the dynamic mechanical response

$$W_{dyn} = \frac{1}{2}E^*(\lambda - 1)^2, \tag{16}$$

where E^* is the dynamic tensile modulus measured at 0.05% strain; this accounts only for the linear mechanical response. W_{dyn} is of the same order of magnitude as the thermal energy, although it is significantly less than the total strain energy, reflecting the contribution of yielding and related structural changes at higher strains. In Fig. 8 the storage, E', and loss, E'', moduli are plotted as a function of temperature; these are consistent with previous dynamic mechanical results [7,9,42]. Assuming the data approximate equilibrium conditions, the decrease in the moduli with temperature implies that the mechanical response at very low strains cannot be purely entropic [31,34,38,43].

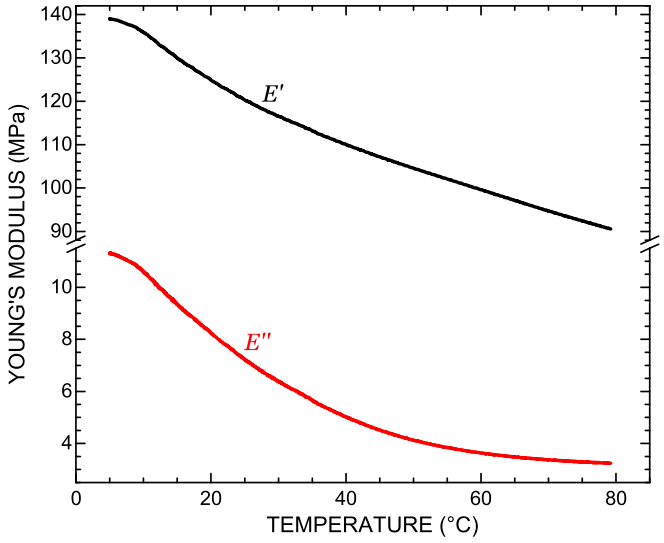

Fig. 8. Dynamic moduli of the polyurea measured at 1 Hz and 0.05% strain.

5. Concluding remarks

The response of polyurea to mechanical perturbation is strongly rate dependent and associated with substantial energy loss. This unusual degree of viscoelasticity is due to a high glass transition temperature and large internal friction, the latter a consequence of the polarity of the chain segments and their extensive hydrogen-bonding. Beyond the linear regime, the phase-segregated morphology of the material, characterized by nano-domains interconnected with the soft matrix, is perturbed by strain, amplifying the strain energy. The resulting temperature changes in turn affect the mechanical response. This rich mechanical behavior underlies many applications of polyurea elastomers, but also complicate efforts to analyze and predict the mechanical properties.

One important application for polyurea is as an impact coating. For ballistic impact, it has been calculated that about 4 GJ/m^3 is consumed by the coating during penetration by a projectile [5,3], which far exceeds the values in Fig. 6. This discrepancy is due to the large difference in strain rates. Ballistic impact is orders of magnitude faster than the measurements herein, sufficiently fast to induce a transition of the polymer to the glassy state [3,6]. The glass transition zone is associated with the largest energy dissipation achievable with a rubbery polymer. Interestingly, recent results [44] suggest that a highly dissipative polymer such as polyurea can be effective as a ballistic coating even in the absence of any strain-induced phase transition.

Acknowledgement

D.A. Rosenberg expresses his gratitude for a National Research Council Postdoctoral Research Associateship at the Naval Research Laboratory. This work was supported by the Office of Naval Research, in part by Code 332 (R.G.S. Barsoum).

References

[1] S.S. Sarva, S. Deschanel, M.C. Boyce, W. Chen, Stress-strain behavior of a polyurea and a polyurethane from low to high strain rates, Polymer 48 (2007) 2208, http://dx.doi.org/10.1016/j.polymer.2007.02.058.

[2] C.M. Roland, J.N. Twigg, Y. Vu, P.H. Mott, High strain rate mechanical behavior of polyurea, Polymer 48 (2007) 574, http://dx.doi.org/10.1016/j.polymer.2006.11.051.

[3] R.B. Bogoslovov, C.M. Roland, R.M. Gamache, Impact-induced glass transition in elastomeric coatings, Appl. Phys. Lett. 90 (2007) 221910, http://dx.doi.org/10.1063/1.2745212.

[4] Z. Xue, J.W. Hutchinson, Neck development in metal/elastomer bilayers under dynamic stretchings, Int. J. Solids Struct. 45 (2008) 3769, http://dx.doi.org/10.1016/j.ijsolstr.2007.10.006.

[5] C.B. Giller, R.M. Gamache, K.J. Wahl, A.P. Saab, C.M. Roland, Coating/substrate interaction in elastomer-steel bilayer armor, J. Compos. Mater. (2016), http://dx.doi.org/10.1177/0021998315613131 (in press).

[6] M. Grujicic, B. Pandurangan, T. He, B.A. Cheeseman, C.F. Yen, C.L. Randow, Computational investigation of impact energy absorption capability of polyurea coatings via deformation-induced glass transition, Mater. Sci. Eng. A 527 (2010) 7741, http://dx.doi.org/10.1016/j.msea.2010.08.042.

[7] R.G. Rinaldi, M.C. Boyce, S.J. Weigand, D.J. Londono, M.W. Guise, Microstructure evolution during tensile loading histories of a polyurea, J. Polym. Sci. B Polym. Phys. 49 (2011) 1660, http://dx.doi.org/10.1002/polb.22352.

[8] T. Choi, D. Fragiadakis, C.M. Roland, J. Runt, Microstructure and segmental dynamics of polyurea under uniaxial deformation, Macromolecules 45 (2012) 3581, http://dx.doi.org/10.1021/ma300128d.

[9] J.A. Pathak, J.N. Twigg, K.E. Nugent, D.L. Ho, E.K. Lin, P.H. Mott, C.G. Robertson, M.K. Vukmir, T.H. Epps III, C.M. Roland, Structural evolution in a polyurea segmented block copolymer because of mechanical deformation, Macromolecules 41 (2008) 7534, http://dx.doi.org/10.1021/ma8011009.

[10] S.L. Dart, R.L. Anthony, E. Guth, Rise of temperature on fast stretching of synthetics and natural rubbers, Ind. Eng. Chem. 34 (1942) 1340, http://dx.doi.org/10.1021/ie50395a020.

[11] J.C. Mitchell, D.J. Meier, Rapid stress-induced crystallization in natural rubber, J. Polym. Sci. A 2 (6) (1968) 1689, http://dx.doi.org/10.1002/pol.1968.160061001.

[12] V. Kerchman, C. Shaw, Experimental study and finite element simulation of heat build-up in rubber compounds with application to fracture, Rubber Chem. Technol. 76 (2003) 386, http://dx.doi.org/10.5254/1.3547750.

[13] J.-B. Le Cam, A review of the challenges and limitations of full-field measurements applied to large heterogeneous deformations of rubbers, Strain 48 (2012) 174, http://dx.doi.org/10.1111/j.1475-1305.2011.00830.x.

[14] J.-B. Le Cam, E. Toussaint, O. Dubois, Effect of thermal cycles on the deformation state at the crack tip of crystallizable natural rubber, Strain 48 (2012) 153, http://dx.doi.org/10.1111/j.1475-1305.2011.00807.x.

[15] T. Pottier, M.-P. Moutrille, J.-B. Le Cam, X. Balandraud, M. Grédiac, Study on the use of motion compensation techniques to determine heat sources. Application to large deformations on crack rubber specimens, Exp. Mech. 49 (2009) 561, http://dx.doi.org/10.1007/s11340-008-9138-0.

[16] D. Guyomar, Y. Li, G. Sebald, P.-J. Cottinet, B. Ducharne, J.-F. Capsal, Elastocaloric modeling of natural rubber, Appl. Therm. Eng. 57 (2013) 33, http://dx.doi.org/10.1016/j.applthermaleng.2013.03.032.

[17] Z. Xie, G. Sebald, D. Guyomar, Elastocaloric effect dependence on pre-elongation in natural rubber, Appl. Phys. Lett. 107 (2015) 081905, http://dx.doi.org/10.1063/1.4929395.

[18] J.R. Samaca Martinez, J.-B. Le Cam, X. Balandraud, E. Toussaint, J. Caillard, "Mechanisms of deformation in crystallizable natural rubber. Part 1: thermal characterization, Polymer 54 (2013) 2717, http://dx.doi.org/10.1016/j.polymer.2013.03.011.

[19] J.R. Samaca Martinez, J.-B. Le Cam, X. Balandraud, E. Toussaint, J. Caillard, "Mechanisms of deformation in crystallizable natural rubber. Part 2: quantitative calorimetric analysis, Polymer 54 (2013) 2727, http://dx.doi.org/10.1016/j.polymer.2013.03.012.

[20] J.-B. Le Cam, J.R. Samaca Martinez, X. Balandraud, E. Toussaint, J. Caillard, Thermomechanical analysis of the singular behavior of rubber: entropic elasticity, reinforcement by fillers strain-induced crystallization and the Mullins effect, Exp. Mech. 55 (2015) 771, http://dx.doi.org/10.1007/s11340-014-9908-9.

[21] M.P. Votinov, E.V. Kuvshinskiĭ, Thermoelastic phenomena in SKS-30A and SKB rubber compounds in adiabatic deformation, Rubber Chem. Technol. 32 (1959) 1016, http://dx.doi.org/10.5254/1.3542461.

[22] V. Le Saux, Y. Marco, S. Calloch, P. Charrier, Contributions of accurate thermal measurements to the characterization of thermomechanical properties of rubber-like materials, Plast., Rubber Compos. 41 (2012) 277, http://dx.doi.org/10.1179/1743289812Y.0000000015.

[23] D. Fragiadakis, R. Gamache, R.B. Bogoslovov, C.M. Roland, Segmental dynamics of polyurea: effect of stoichiometry, Polymer 51 (2010) 178, http://dx.doi.org/10.1016/j.polymer.2009.11.028.

[24] P.H. Mott, J.N. Twigg, D.F. Roland, H.S. Schrader, J.A. Pathak, C.M. Roland, High Speed Tensile Test instrument." Review of Scientific Instruments vol. 78, 2007, p. 0145105, http://dx.doi.org/10.1063/1.2719643.

[25] C.M. Roland, R. Casalini, Effect of hydrostatic pressure on the viscoelastic response of polyurea, Polymer 48 (2007) 5747–5752.

[26] K. Holzworth, Z. Jia, A.V. Amirkhizi, J. Qiao, S. Nemat-Nasser, Effect of isocyanate content on thermal and mechanical properties of polyuria, Polymer 54 (2013) 3079, http://dx.doi.org/10.1016/j.polymer.2013.03.067.

[27] T.L. Bergman, A.S. Lavine, F.P. Incropera, D.P. DeWitt, Fundamentals of Heat and Mass Transfer, seventh ed., Wiley, Hoboken NJ, 2011.

[28] H.D. Baehr, K. Stephan, Heat and Mass Transfer, third ed., Springer-Verlag, Berlin, 2011 [Chapter 2].

[29] C.J.M. Lasance, The Thermal Conductivity of Rubber/elastomers, November 2001. Electronics Cooling, http://www.electronics-cooling.com/2001/11/the-thermal-conductivity-of-rubbers-elastomers/. accessed 10 May 2016.

[30] K. Akutagawa, S. Hamatani, T. Nashi, The new interpretation for the heat build-up phenomena of rubber materials during deformation, Polymer 66 (2015) 201, http://dx.doi.org/10.1016/j.polymer.2015.04.040.

[31] R.L. Anthony, R.H. Caston, E. Guth, "Equations of state for natural and synthetic rubber-like materials. I. Unaccelerated natural soft rubber, J. Phys. Chem. 46 (1942) 826, http://dx.doi.org/10.1021/j150422a005.

[32] P.J. Flory, Principles of Polymer Chemistry, Cornell University Press, Ithaca, 1953 [Chapter 11].

[33] G.A. Holzapfel, J.C. Simo, Entropy elasticity of isotropic rubber-like solids at finite strains, Comput. Methods Appl. Mech. Eng. 132 (1996) 17, http://dx.doi.org/10.1016/0045-7825(96)01001-8.

[34] L.R.G. Treloar, The Physics of Rubber Elasticity, third ed., Oxford University Press, Oxford, 1975 [Chapter 2].

[35] M. Biron, Thermoset and Composites: Technical Information for Plastics Users, Elsevier, Oxford, 2004 [table 4.11].

[36] Y.K. Godovsky, Calorimetric study of rubber elasticity, Polymer 22 (1981) 75, http://dx.doi.org/10.1016/0032-3861(81)90080-X.

[37] F. Kremer, A. Schönhals, The scaling of the dynamics of glasses and supercooled liquids, in: F. Kremer, A. Schönhals (Eds.), Broadband Dielectric Spectroscopy, Springer-Verlag, Berlin, 2003 [Chapter 4].

[38] C.M. Roland, Viscoelastic Behavior of Rubbery Materials, Oxford University Press, Oxford, 2011 [Chapter 4].

[39] In strict terms, W_{strain} and W_{recv} should be calculated from adiabatic stress-strain curves. However, the deviation from adiabatic only becomes important at low rates, where both the temperature increases, and its adiabatic correction, are small (~2.5 °C). Fig. 8 shows that Young's modulus decreases by ~2% as the temperature is increased from 25 to 28 °C. To a first approximation, W_{strain} and W_{recv} found herein will differ from their adiabatic values by a similar fraction. Thus, the error introduced by this assumption is smaller than the scatter shown in the strain energy balance plotted in Fig 6.

[40] G. Allen, C. Price, N. Yoshimura, Thermomechanical studies on natural rubber in torsion and simple extension, J. Chem. Soc. Faraday Trans. 71 (1975) 548, http://dx.doi.org/10.1039/F19757100548.

[41] G. Allen, C. Price, N. Yoshimura, Thermomechanical heat of deformation studies on *cis*-polybutadiene, Polymer 16 (1975) 261, http://dx.doi.org/10.1016/0032-3861(75)90167-6.

[42] J. Zhao, W.G. Knauss, G. Ravichandran, Applicability of the time–temperature superposition principle in modeling dynamic response of a polyurea, Mech. Time Depend. Mater. 11 (2007) 289, http://dx.doi.org/10.1007/s11043-008-9048-7.

[43] B. Erman, J.E. Mark, Structures and Properties of Rubberlike Networks, Oxford University Press, Oxford, 1997 [Chapter 9].

[44] R.M. Gamache, C.B. Giller, G. Montella, D. Fragiadakis, C.M. Roland, Elastomer-metal laminate armor, Mater. Des. 111 (2016) 362, http://dx.doi.org/10.1016/j.matdes.2016.08.072.